Investigating the Mechanical Properties of 2D Materials with Structures 1T-MX2 (M=Ti, V; X=S, Se, Te) through the Atomic Finite Element Method

NGUYEN HUU TU[1], NGUYEN VAN THANH[1], DO XUAN KIEN[1], NGUYEN VAN TRANG[2], VU QUOC HIEN[3], TRAN NGOC GIANG[2,*]

[1]Faculty of Fundamental Science,
Military Academy of Logistics,
Ha Noi,
VIETNAM

[2]Faculty of Mechanical Engineering,
Thai Nguyen University of Technology,
Thai Nguyen,
VIETNAM

[3]Viet Tri University of Industry,
Phu Tho,
VIETNAM

[*]*Corresponding Author*

Abstract: - In this study, the mechanical characteristics of two-dimensional materials Titanium 1T-TiX_2 and Vanadium 1T-VX_2 (X=S, Se, Te) were determined by the atomic finite element method (AFEM). The Stillinger-Welber potential function was used to describe the binding potential of the atoms in the tensile test simulation of these materials. The results determined the mechanical characteristics of the materials: the two-dimensional elastic modulus $E.t$ has a value in the range of 40.98÷86.84 N/m; the Poisson's ratio is in the range of 0.418÷0.234; the maximum stress $\sigma.t$ is in the range of 4.75÷13.02 and the strain at maximum stress ε is in the range of 21.3%÷31.3%. The study also showed that the two-dimensional elastic modulus when stretched in the zigzag direction (ZZ) is approximately equal to that when stretched in the armchair direction (AC), so these materials can be considered isotropic. These results provide a basis for their practical applications such as electronics, spintronics, and energy-related fields.

Key-Words: - 2D elastic modulus, Mechanical characterization, 2D material, 1T-VX_2, 1T-TiX_2, AFEM.

Received: January 19, 2026. Revised: March 25, 2026. Accepted: April 21, 2026. Published: August 4, 2026.

1 Introduction

Figure 1 shows the structure of the 1T-MX_2 materials. On the orthogonal projection of the sheet surface, the material structure consists of two interlocking hexagonal lattices with 3 out of 6 vertices coinciding; this structure is different from the planar hexagonal structure of Graphene sheets [1] and the low-buck structure of Silicenere, BN [2]. In the 1T-MX_2 structure, M is a metal (Ti and V) and X is a non-metal (S, Se, and Te); it likes 1 T structure in [3], [4]; Each basic cell (the dashed rectangle in Figure 1) has a side length of a ($\mathring{A}$), containing 9 atoms: 3 metal atoms M (red) located on one plane and 6 non-metal atoms X = S, Se, and Te (blue) distributed on two planes symmetrical with respect to the plane containing metal M. Throughout the entire sheet, each metal atom M is bonded to 6 non-metal atoms X; the distance between the plane containing the metal and the non-metal is h (side projection); correspondingly, each non-metal atom X (S, Se, Te) is bonded to 3 surrounding metal atoms M. To fully determine the structure of these sheets, the following material parameters need to be known: the bond distance between the metal atom M (Ti and V) and the non-metal atom X (S, Se, and Te) is d_{M-X}; The bond angle between X-M-X atoms is θ_{XMX}, and between M-X-M atoms is θ_{MXM}, lattice constant a. All these

parameters for the six 1T-MX_2 materials are given in Table 1.

Materials such as 1T-MX_2 , 1T-TiX_2 and 1T-VX_2 possess many novel and unique physical properties. The ferroelectricity in the charge density wave (CDW) material 1*T*-TiX_2 (*X*=S, Se, and Te) bilayers by stacking two van der Waals monolayers was studied by the first-principles calculations, [5]. The dependence of the magnetic states of the untwisted and twisted bilayer 1T-VX_2 (*X*=S, Se) on the interlayer distance was determined by density functional theory calculations, [6]. Magnetism can be tuned through changes in crystal phase (e.g., from 1T to 2H), changes in defect concentration, or through mechanical deformation. Charge Density Wave (CDW) is a characteristic quantum physical phenomenon that occurs when electrons in a crystal lattice reorganize into a periodic wave structure, leading to lattice deformation. CDW is often observed in 2D transition metals. Applications: Controlling CDW opens the door to high-speed switching devices and memory devices. Optical properties can be tuned by changing layer thickness or creating heterostructures, allowing for fine-tuning of the interaction between matter and light. Superconductivity can be adjusted by interleaving atoms between layers or by strain engineering. The 2D metallic VX_2 (VX_2, X =S, Se, and Te) materials and related heterostructures in the aspects of their structures, fabrication methods, key properties, and potential applications, [7]. The electronic and optical properties of titanium dichalcogenide materials TiX_2 (X=S, Se, Te) are calculated by using Quantum Espresso method. The results obtained showed that TiS_2 is a semi metallic compound, this character is due to a very small overlap between the density of states p-orbitals of S and d-orbitals of the Ti atom in the vicinity of the Fermi level. While $TiSe_2$ and $TiTe_2$ indicate the metallic characters, [8].

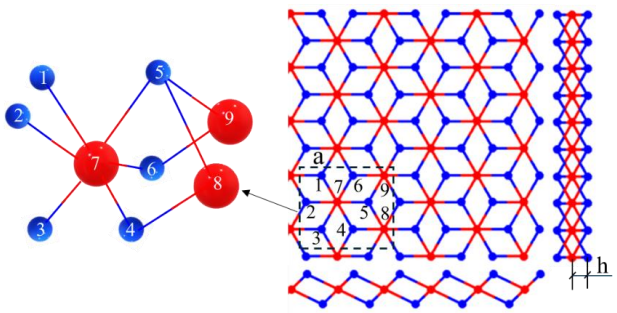

Fig. 1: Material structure of 1T-MX_2 sheets (M are red; X are blue)
Source: created by the authors

Table 1. Material network parameters of 1T-MX_2 sheets (M= Ti, V; X= S, Se and Te)

No.	Materials	Constants a (Å)	d_{M-X} (Å)	θ_{MXM} (°)	θ_{XMX} (°)
1	1T-TiS_2	3.32	2.39	87.984	87.984
2	1T-$TiSe_2$	3.43	2.51	86.199	86.199
3	1T-$TiTe_2$	3.64	2.73	83.621	83.621
4	1T-VS_2	3.10	2.31	84.288	84.288
5	1T-VSe_2	3.24	2.44	83.201	83.201
6	1T-VTe_2	3.46	2.64	81.885	81.885

Source: [9]

Based on its special electrical, magnetic, and structural properties, 1T-MX_2 material promises many applications in the fabrication of Lithium-ion and Sodium-ion super batteries, [10]. To be able to use 1T-MX_2 nanomaterials in practice, a thorough understanding of its mechanical characteristics is needed. Jiang et al. studied the mechanical properties of these 2D materials through molecular dynamics (MD) simulations, [9]. Further studies using other methods are needed to clarify and more fully understand the mechanical properties of this group of materials. Therefore, in this study, we used the atomic finite element method (AFEM) with Stillinger-Weber potential function to calculate the mechanical characteristics of 1T-MX_2 materials. The advantage of the AFEM method is faster computation time while achieving accuracy close to that of MD. The disadvantage is that it does not simulate the material processing basis at varying temperatures like MD, [11].

2 Method

The fundamental problem of the atomic finite element method is to apply the principle of potential minimum to the atomic interaction potential of the 1T-MX_2 sheets (Figure 2). From there, determine the element stiffness matrix, then construct the overall stiffness matrix, and then apply it to the finite element equation:

$$\boldsymbol{K}^{(k)}\boldsymbol{u}^{(k)} = \boldsymbol{F}^{(k)} \tag{1}$$

with

$$\boldsymbol{K}_{ij}^{k} = \frac{\partial^2 \Pi^{(k)}}{\partial \boldsymbol{u}_i \partial \boldsymbol{u}_j}; F_i^{(k)} = -\frac{\partial \Pi^{(k)}}{\partial \boldsymbol{u}_i} = f_i - \frac{\partial E^{(k)}}{\partial \boldsymbol{u}_i} \tag{2}$$

and $\boldsymbol{K}^{(k)}$ being the overall stiffness matrix, $\boldsymbol{u}^{(k)}$ being the nodal displacement vector, and $\boldsymbol{F}^{(k)}$ being the nodal force vector.

Solving the system of equations (2), the displacement of all atoms in the sheet is determined. In the experimental simulation using the atomic finite element method, solving the system of

equations (2) using the Newton-Raphson iterative method, the use of this method is clearly shown in [11], [12], [13], then the equation in finite element form is the form of equation (1). For each 1T-MX_2 sheets, the atomic interaction potential is determined according to the Stillinger-Weber potential function including: the energy of direct binding to the tensile model of two adjacent atoms (E_r, eV) and the energy of binding to the bending model of three adjacent atoms (E_θ, eV) determined by the following energy expressions.

$$E = E_r + E_\theta; E_r = \sum_{i=1}^{m} V_2; E_\theta = \sum_{i=1}^{n} V_3 \quad (3)$$

$$V_2 = Ae^{\lfloor \rho/(r_{ij}-r_{max}) \rfloor} \left(B / r_{ij}^4 - 1 \right) \quad (4)$$

$$V_3 = Ke^{\left[\rho_{ij}/(r_{ij}-r_{max\,ij})+\rho_{ik}/(r_{ik}-r_{max\,ik})\right]} \left(\cos(\theta_{ijk}) - \cos(\theta_0)\right)^2 \quad (5)$$

where E: total atomic bond energy; E_θ (eV): total angular bond energy of 3 atoms on the entire sheet; E_r (eV): total linear bond energy between two atoms of the sheet; V_2(eV): linear bond energy of two adjacent atoms; V_3(eV): angular bond energy of 3 adjacent atoms; m, n: number of linear and angular bonds in a computational model; A(eV), K(eV): material coefficients; ρ(Å), B(Å), ρ_{ij}(Å), ρ_{ik}(Å), θ_o (degrees): geometric parameters of the material; r_{ij} ($Å$), r_{ik} ($Å$): bond lengths between two atoms i, j and k respectively; θ_{ijk} (degrees): bond angle between three atoms i, j, k (where i is the middle atom) (Figure 2).

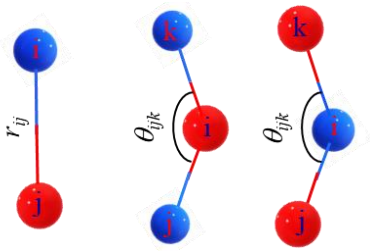

Fig. 2: Element model using Stillinger-Weber potential function: a) Linear bond between two atoms; b, c) Angular bond between three atoms. Red represents metal atom M; Blue represents non-metal atom X

Source: created by the authors

In the tensile experiment simulation, each 1T-MX_2 sheet has a total number of atoms of N; the initial coordinates and displacements of the i-th atom are X_i and u_i respectively; after deformation, the coordinates of the atoms are determined as: $x_i = X_i + u_i$. The atomic interaction potential of the entire sheet calculated by formula (3) is an expression depending on the coordinates of each atom on the sheet as follows:

$$E = E(\boldsymbol{x}_1, \boldsymbol{x}_2, ..., \boldsymbol{x}_N) \quad (6)$$

On the other hand, when the sheet is subjected to an external force f_i on the i-th atom (considered as nodes), the atoms in the sheet have displacements of ui respectively, the potential energy of the external force is calculated as follows:

$$E_{ext} = \sum_{i=1}^{N} \boldsymbol{f}_i \boldsymbol{u}_i \quad (7)$$

On the entire sheet, the total potential energy is:

$$\Pi = E - E_{ext} \quad (8)$$

According to the principle of minimum potential energy, the sheet is in equilibrium when the total potential energy reaches its minimum value. Therefore:

$$\frac{\partial \Pi}{\partial \boldsymbol{u}_i} = 0; \; i = 1 \div N \quad (9)$$

Equation (9) is the equilibrium condition of the sheet. With the total potential energy satisfied (9), the stiffness matrix in equations (1) and (2) is completely determined.

Solve the system of equations (1) using the Newton-Raphson iterative method with boundary conditions on displacement: atoms on the tensile boundary (Figure 3) have displacement equal to u_0; atoms on the holding boundary (Figure 3) have no displacement in the tensile direction. This is the method of simulating the sheet tensile test using the atomic finite element method, thereby determining the mechanical properties of the materials under consideration.

The experimental model for tensile testing of a whole sheet is shown in Figure 3 using the displacement method.

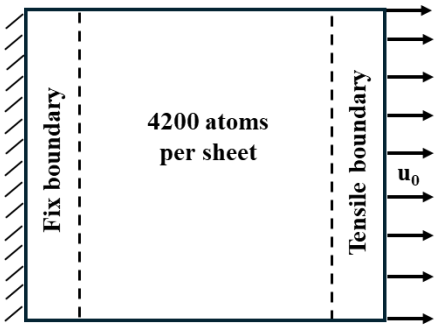

Fig. 3: Boundary conditions for displacement when tensiling the sheets

Source: created by the authors

In the simulation, a rectangular sheet with approximately equal side dimensions is stretched (the rectangle is considered approximately as a square); each sheet has 4200 atoms; In this simulation, the tensile will follow two different directions, zigzag and armchair, corresponding to changes in the fixing and tensiling boundaries along those two directions (Figure 3); each stretching step causes the atoms on the tensile boundary to have a displacement with an increment of δ_ε=0.001, repeated until the bond on the sheet is broken (the bond size is larger than a certain value, at which point the sheet is destroyed); The atoms at the fix boundary have zero position. At each step, solve equation (10) to determine the displacement, calculate the nodal force of all atoms on the sheet at this step. The atomic positions in the following steps are determined as follows:

$$x_{(k+1)} = x_{(k)} + u_{(k)} \quad (10)$$

3 Results and Discussion

The mechanical characteristics of the 1T-MX_2 material sheets (M=Ti, V; X=S, Se, Te) are shown in Table 2 (Appendix). The stress-strain relationships of the six material sheets are shown in Figure 4.

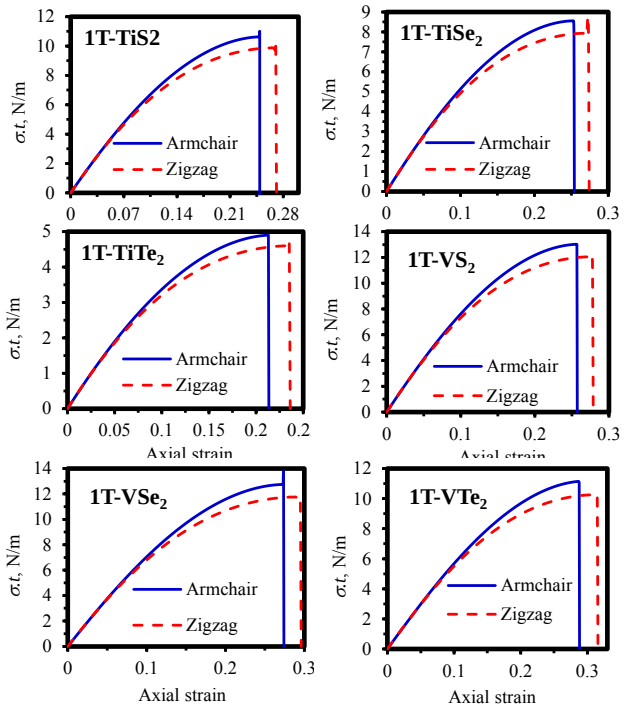

Fig. 4: Stress-strain relationship during tensioning of 1T-MX_2 sheets
Source: created by the authors

Specifically, the two-dimensional elastic modulus *E.t* (N/m) has a value in the range of 40.98 ÷ 86.84 N/m; the Poisson's ratio has a value in the range of 0.148 ÷ 0.234; the maximum two-dimensional stress ($\sigma.t_{max}$) when stretched is in the range of 4.75 ÷ 13.02 N/m; the strain at maximum stress is in the range of 21.3% to 31.3%. In Table 2 (Appendix), the calculated results were compared with the research results of [9] with the same experimental simulation conditions. The comparison results show that the error is not large, specifically: the error of the elastic modulus is in the range of -1.57% to 1.03%; the error of the Poisson's ratio is from -9.05% to 0.67%; The maximum two-dimensional stress error during tension ranges from -6.64% to 1.06%; the maximum stress strain error ranges from -8.62% to 1.00%. The failure of the sheet occurs when the bonds between adjacent atoms are broken. Figure 5 shows the failure of the 1T-TiS_2 sheet when pulled in the armchair direction with a strain ε = 0.2495; when pulled in the zigzag direction, at a step of ε = 0.27. In both cases, local deformation occurred before complete failure; subsequently, many bonds on the sheet were broken, rendering it incapable of withstanding the force, and the sheet completely failed (Figure 5).

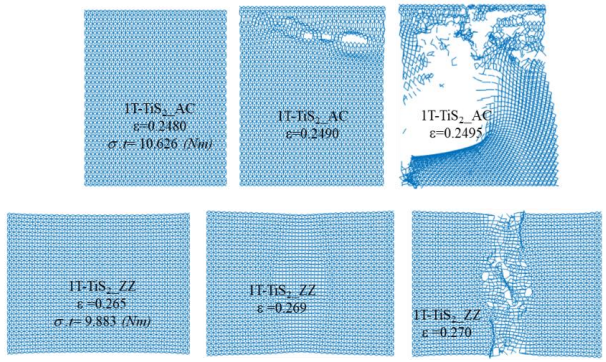

Fig. 5: Tensile fracture of 1T-TiS_2 sheets
Source: created by the authors

4 Conclusion

In this study, the mechanical properties of six two-dimensional orthosymmetric 1T-MX_2 materials (M=Ti, V; X=S, Se, Te) were determined using the atomic finite element method with Stillinger-Weber potential functions. The results showed that these materials have two-dimensional elastic moduli and Poisson's ratios that are approximately equal under armchair and zigzag tension. From these calculations, they can be considered approximately isotropic materials. The determined mechanical characteristics form the basis for calculating other

mechanical parameters of the materials, such as fracture studies and the determination of natural vibration frequencies. These are important studies that will contribute to the practical application of 1T-MX_2 nanomaterials. These results can be used as a reference and a basis for applying this nanomaterial in the design and fabrication of batteries, electronic devices, semiconductors, and many other fields. The limitation of this study is that it does not consider the influence of defects on the mechanical behavior of the plate. This will be clarified in subsequent studies.

Acknowledgement:
Military Academy of Logistics and Thai Nguyen University of Technology supported this work.

References:

[1] Geim, A.K., Graphene: status and prospects. science, 2009. 324(5934): p. 1530-1534. https://doi.org/10.1126/science.1158877.

[2] Nguyen, H.-T., M.-Q. Le, and V.-T. Nguyen, Mode-I stress intensity factors of silicene, AlN, and SiC hexagonal sheets. Materials Research Express, 2018. 5(6): p. 065025. https://doi.org/10.1088/2053-1591/aac807.

[3] Ogunkunle, S. A., Bouzid, A., Hinsch, J. J., Allen, O. J., White, J. J., Bernard, S., ... & Wang, Y., Defect engineering of 1T′ MX_2 (M= Mo, W and X= S, Se) transition metal dichalcogenide-based electrocatalyst for alkaline hydrogen evolution reaction. Journal of Physics: Condensed Matter, 2024. 36(14): p. 145002. https://doi.org/10.1088/1361-648X/ad19a4.

[4] Staros, D., B. Rubenstein, and P. Ganesh, A first-principles study of bilayer 1 T'-WTe_2/CrI_3: a candidate topological spin filter. npj Spintronics, 2024. 2(1): p. 4. https://doi.org/10.1038/s44306-023-00007-y.

[5] Liu, Y., Wang, S., Wu, Y., Li, F., & Wang, L., Ferroelectricity in charge-density-wave 1T-TiX_2 (X= S, Se, and Te) bilayers. Physical Review B, 2025. 111(2): p. 024101. https://doi.org/10.1103/PhysRevB.111.024101

[6] Qiao, L. Y., Jiang, X. C., Ruan, Z., & Zhang, Y. Z., Tunable magnetism in bilayer transition metal dichalcogenides. Physical Review Materials, 2024. 8(3): p. 034003. https://doi.org/10.1103/PhysRevMaterials.8.034003.

[7] Hossain, M., Zhang, H., Huangfu, Y., Saeed, M. Z., Qin, B., Bloos, D., & Duan, X., 2D metallic vanadium dichalcogenides and related hetero-structures. Materials Today Advances, 2024. 21: p. 100451. https://doi.org/10.1016/j.mtadv.2023.100451..

[8] Hossain, M., Zhang, H., Huangfu, Y., Saeed, M. Z., Qin, B., Bloos, D., & Duan, X., Theoretical investigation of optoelectronics properties of titanium dichalcogenides materials TiX_2 (X= S, Se, Te) using quantum espresso. in Materials Science Forum. 2023. Trans Tech Publ. https://doi.org/10.4028/p-erZ4kn.

[9] Jiang, J.-W., Handbook of Stillinger-Weber potential parameters for two-dimensional atomic crystals, 2017. ISBN: 978-953-51-3696-5.

[10] Santra, S., Ali, M. S., Karmakar, S., & Chattopadhyay, D., Molybdenum disulfide: A nanomaterial that is paving the way toward a sustainable future. Materials Today Sustainability, 2023. 25: p. 100659. https://doi.org/10.1016/j.mtsust.2023.100659.

[11] Liu, B., Huang, Y., Jiang, H., Qu, S., & Hwang, K. C., The atomic-scale finite element method. Computer methods in applied mechanics and engineering, 2004. 193(17-20): p. 1849-1864. https://doi.org/10.1016/j.cma.2003.12.037.

[12] Wang, Y., Zhang, C., Zhou, E., Sun, C., Hinkley, J., Gates, T. S., & Su, J., Atomistic finite elements applicable to solid polymers. Computational materials science, 2006. 36(3): p. 292-302. https://doi.org/10.1016/j.commatsci.2005.03.016.

[13] Wackerfuß, J., Molecular mechanics in the context of the finite element method. International Journal for Numerical Methods in Engineering, 2009. 77(7): p. 969-997. https://doi.org/10.1002/nme.2442.

APPENDIX

Table 2. Mechanical parameters of the 1T-MX_2 material sheets

No.	Materials	Directions	*E.t* (*N/m*)			ν			(σ.t) (*Nm*)			ε		
			Our result	[9]	Error %	Our result	[9]	Error %	Our result	[9]	Error %	Oresult	[9]	Error%
1	1T-TiS_2	AC	73.82	75	-1.57	0.194	0.2	-3.00	10.63	10.8	-1.57	0.248	0.25	-0.80
		ZZ	74.65	74.6	0.07	0.192	0.2	-4.00	9.88	10.4	-5.00	0.265	0.29	-8.62
2	1T-$TiSe_2$	AC	58.53	59.2	-1.13	0.197	0.2	-1.50	8.55	8.7	-1.72	0.252	0.25	1.00
		ZZ	59.29	58.9	0.66	0.195	0.2	-2.50	7.93	8.3	-4.46	0.270	0.29	-6.90
3	1T-$TiTe_2$	AC	40.98	41.4	-1.01	0.151	0.15	0.67	4.91	4.9	0.20	0.213	0.22	-3.18
		ZZ	41.28	41.2	0.19	0.148	0.15	-1.33	4.75	4.7	1.06	0.235	0.25	-6.00
4	1T-VS_2	AC	85.81	87.1	-1.48	0.204	0.21	-2.86	13.02	13.3	-2.11	0.256	0.26	-1.35
		ZZ	86.84	86.8	0.05	0.191	0.21	-9.05	12.19	12.7	-4.02	0.277	0.30	-7.67
5	1T-VSe_2	AC	77.81	78.4	-0.75	0.218	0.22	-0.91	12.75	13.1	-2.67	0.272	0.27	0.74
		ZZ	78.82	78.1	0.92	0.215	0.22	-2.27	11.84	12.5	-5.28	0.294	0.32	-8.12
6	1T-VTe_2	AC	60.73	61.2	-0.77	0.234	0.24	-2.50	11.14	11.5	-3.13	0.287	0.30	-4.33
		ZZ	61.63	61.0	1.03	0.231	0.24	-3.75	10.27	11.0	-6.64	0.313	0.34	-7.94

Source: created by the authors

Contribution of Individual Authors to the Creation of a Scientific Article (Ghostwriting Policy)

The authors equally contributed to the present research, at all stages from the formulation of the problem to the final findings and solution.

Sources of Funding for Research Presented in a Scientific Article or the Scientific Article Itself

Military Academy of Logistics and Thai Nguyen University of Technology supported this work.

Conflict of Interest

The authors have no conflicts of interest to declare that are relevant to the content of this article.